

Rhodamine B dye biosorption using babassu coconut mesocarp: batch and dynamic studies

In this study, biosorption of Rhodamine B (RhB) dye from aqueous solution using babassu coconut mesocarp (BCM) was evaluated in batch and continuous operation. The influence of pH, contact time, biosorbent dosage, dye concentration, and temperature were investigated in batch studies. Higher removal rates of RhB ($79.3 \pm 0.49\%$) were obtained at pH 2. The kinetic and equilibrium studies indicated that the biosorption follows the pseudo-second-order model and Langmuir isotherm model. The maximum biosorption capacity was estimated at 111.52 mg g^{-1} (at 40°C). According to Dubinin–Radushkevich (DR) isotherm model, biosorption of RhB onto BCM was found to be physical. The thermodynamic parameters ($\Delta G < 0$ and $\Delta H > 0$) suggested that the biosorption process was spontaneous and facilitated with the rise in temperature (endothermic). Continuous study was conducted in an up-flow fixed-bed column fed with 50 mg L^{-1} RhB solution at a flow rate of 4 mL/min . Yan and Yoon-Nelson models described the breakthrough data with excellent accuracy. The maximum uptake of fixed-bed column and the breakthrough time were reported as 72.45 mg g^{-1} and 611 min , respectively. It can be concluded that BCM is an attractive biosorbent for the remediation of RhB from the aqueous phase.

Keywords: Dye removal; Kinetic; Isotherms; Fixed-bed column; Thermodynamic study.

Biossorção do corante Rodamina B por mesocarpo do coco do babaçu: estudo em batelada e em coluna

Neste estudo, a biossorção do corante Rodamina B (RhB) de solução aquosa usando mesocarpo do coco do babaçu (BCM) foi avaliada em batelada e operação contínua. As influências do pH, tempo de contato, concentração do biossorvente, concentração de corante e temperatura foram investigadas em estudos de batelada. Taxas mais altas de remoção de RhB ($79,3 \pm 0,49\%$) foram obtidas em pH 2.0. Os estudos cinéticos e de equilíbrio indicaram que a biossorção segue o modelo de pseudosegunda ordem e o modelo de isoterma de Langmuir, respectivamente. A capacidade máxima de biossorção do BCM foi estimada em $111,52 \text{ mg g}^{-1}$ a 40°C . De acordo com o modelo de isotermas de Dubinin–Radushkevich (DR), a biossorção da RhB pelo BCM é um processo físico. Os parâmetros termodinâmicos ($\Delta G < 0$ e $\Delta H > 0$) sugeriram que o processo de biossorção é espontâneo e facilitado com o aumento da temperatura (endotérmico). O estudo contínuo foi realizado em uma coluna de leito fixo de fluxo ascendente alimentada com solução de RhB de 50 mg L^{-1} e vazão de 4 mL min^{-1} . Os modelos de Yan e Yoon-Nelson descreveram os dados experimentais da curva de ruptura com excelente precisão. A captação máxima da coluna de leito fixo e o tempo de ruptura foram determinados como $72,45 \text{ mg g}^{-1}$ e 611 min , respectivamente. Conclui-se que o BCM é um biossorvente atraente para a remediação de RhB de fase aquosa.

Palavras-chave: Remoção de corante; Cinética; Isotermas; Coluna de leito fixo; Estudo termodinâmico.

Topic: Engenharia Sanitária

Received: 02/02/2022

Approved: 24/02/2022

Reviewed anonymously in the process of blind peer.

Eduardo Beraldo de Morais 
Universidade Federal de Mato Grosso, Brasil
<http://lattes.cnpq.br/2910407574938593>
<http://orcid.org/0000-0002-8505-4133>
beraldo_morais@yahoo.com.br

Leonardo Gomes de Vasconcelos 
Universidade Federal de Mato Grosso, Brasil
<http://lattes.cnpq.br/6010413631026964>
<http://orcid.org/0000-0002-2886-1887>
vasconceloslg@gmail.com

Frederico Carlos Martins de Menezes Filho 
Universidade Federal de Viçosa, Brasil
<http://lattes.cnpq.br/6934146250991610>
<http://orcid.org/0000-0003-4874-0254>
frederico.menezes@ufv.br

Danila Soares Caixeta 
Universidade Federal de Mato Grosso, Brasil
<http://lattes.cnpq.br/8314296350945580>
<http://orcid.org/0000-0002-2036-1378>
danilacaixeta@gmail.com

Evandro Luiz Dall'Oglio 
Universidade Federal de Mato Grosso, Brasil
<http://lattes.cnpq.br/0288804659104012>
<http://orcid.org/0000-0002-8936-5107>
dalloglio.evandro@gmail.com

Rosseean Golin 
Universidade Federal de Mato Grosso, Brasil
<http://lattes.cnpq.br/4684005974138067>
<http://orcid.org/0000-0001-9065-1023>
golin.rosseean@gmail.com

Alessandra Lima Deluque 
Universidade Federal de Mato Grosso, Brasil
<http://lattes.cnpq.br/3377049548276218>
<http://orcid.org/0000-0002-4042-6028>
alessandralima042@hotmail.com

Aldecy de Almeida Santos 
Universidade Federal de Mato Grosso, Brasil
<http://lattes.cnpq.br/3224921282419849>
<http://orcid.org/0000-0003-4361-307X>
aldecy_allmeida@yahoo.com.br



DOI: 10.6008/CBPC2179-6858.2022.002.0009

Referencing this:

MORAIS, E. B.; VASCONCELOS, L. G.; MENEZES FILHO, F. C. M.; CAIXETA, D. S.; DALL'OGGIO, E. L.; GOLIN, R.; DELUQUE, A. L.; SANTOS, A. A.. Rhodamine B dye biosorption using babassu coconut mesocarp: batch and dynamic studies. *Revista Ibero Americana de Ciências Ambientais*, v.13, n.2, p.90-103, 2022. DOI: <http://doi.org/10.6008/CBPC2179-6858.2022.002.0009>

INTRODUCTION

Synthetic dyes are widely used in the textile, plastic, rubber, paper, tanneries, and paint industries. These produce large amounts of wastewater containing high concentrations of dyes (up to 250 mg/L) that are often discharged into water bodies (SEGURA et al., 2016; KOOH et al., 2016). In the aquatic ecosystems, the dyes cause aesthetic problems, reduce light penetration and photosynthesis, and lead to a depletion of dissolved oxygen (CASTRO et al., 2017). Besides, most of the dyes and their metabolites are potentially toxic, mutagenic, and carcinogenic to animals, plants, microalgae, protozoa, and bacteria (NOVOTNÝ et al., 2006).

In the recent decade, the treatment of dye-containing wastewaters has been extensively studied and tested. Many chemical, physical and biological technologies such as electrocoagulation and catalytic ozonation (TANVEER et al., 2022), color irradiation (PARVIN et al., 2015), nanofiltration (LIU et al., 2017), activated sludge (GEBRATI et al., 2019), and constructed wetlands (SETHULEKSHMI et al., 2021), have been used. However, large-scale applications of these techniques are expensive, require high-tech operations and skilled personnel, and can produce large amounts of sludge as well as toxic compounds (SANTAEUFEMIA et al., 2018). On the other hand, adsorption has become well-established technology to remove different pollutants, including dyes, from water and wastewater (SANTOS et al., 2019). The simplicity of design, low operational cost, high efficiency in treating wastewaters with a low or high concentration of pollutants make the adsorption a techno-economically viable solution (CASTRO et al., 2017; TEIXEIRA et al., 2021).

Among different adsorbents used to remove dyes from aqueous media, biomasses have gained considerable attention because they are plentiful in nature, or are by-products or wastes from the agro-industrial activities, and have low or no economic value (TUNÇ et al., 2009). Several biomasses have been applied in the dye adsorption including *Casuarina equisetifolia* needles (KOOH et al., 2016), jujube shell (EL MESSAOUDI et al., 2016), forestry waste mixture (pine, oak, hornbeam, and fir sawdust) (DENIZ et al., 2017), yeast slurry from brewery (CASTRO et al., 2017), microalgae (DANESHVAR et al., 2017), bean husks (BELLO et al., 2019) and sugarcane bagasse (FIDELES et al., 2019).

Babassu (*Orbignya speciosa*) is an abundant palm tree found mainly in the north-central region of Brazil, which produces fruits in an ellipsoidal form (VIEIRA et al., 2011). From this fruit, nuts are extracted, and a fibrous lignocellulosic by-product, named babassu coconut mesocarp (BCM), is produced. Similar to other lignocellulosic materials, BCM has different functional groups on the surface of the cell wall, making it interesting to evaluate the feasibility of dye adsorption. Recently, the use of BCM on adsorption of acetylsalicylic acid and copper ions was demonstrated (NASCIMENTO et al., 2019; HOPPEN et al., 2019).

In this study, Rhodamine B (RhB) was used as a model dye during the evaluation of the BCM adsorption performance in aqueous solution. RhB belongs to the xanthene class of dyes and is widely used in textiles, paint, leather, and paper industries (KOOH et al., 2016). However, it is considered a toxic substance and harmful to organisms (TRIPATY et al., 1995). In humans, RhB can cause acute irritation to the skin, eyes, and respiratory tract (TAN et al., 2014). Therefore, this dye should be removed from wastewater before its disposal. Here, we investigated the adsorption of RhB by BCM under different experimental conditions. The

factors evaluated were pH, contact time, biosorbent dosage, dye concentration, and temperature. Adsorption kinetics, isotherms, and thermodynamic parameters were also determined, and RhB removal mechanisms were explored by Fourier transform infrared spectroscopy (FTIR). Furthermore, the biosorption of RhB in continuous systems was evaluated in an up-flow fixed-bed column.

MATERIALS AND METHODS

Reagents

Rhodamine B (molecular formula: $C_{28}H_{31}ClN_2O_3$, molecular weight: $479.01 \text{ g mol}^{-1}$, CAS number: 81-88-9) was supplied by Sigma Aldrich – Brazil. A stock solution of RhB (1.0 g L^{-1}) was prepared by dissolving the dye in distilled water. The experimental solutions with concentration of RhB ranging from 20 to 200 mg L^{-1} were obtained by diluting the stock solution. 0.1 M HCl and 0.1 M NaOH solutions were used for adjusting the pH of the experimental solutions. HCl and NaOH were of analytical grade.

Biosorbent

Babassu coconut was collected in the city of Santo Antônio do Leverger, Mato Grosso state, in the midwestern region of Brazil. The mesocarp of the raw babassu coconut was cut in small pieces, washed with abundant distilled water to remove soluble impurities and dirt, and dried in an oven at $80 \text{ }^\circ\text{C}$ for 48 h. After that, dry BCM was ground to a fine powder using a steel-knife electrical mill, sieved through a $149 \text{ }\mu\text{m}$ standard sieve, and then stored in desiccators until use.

The point of zero charge (pH_{PZC}) of BCM was determined by the salt addition method (DAHRI et al., 2014). The experiment was conducted in a series of 100 mL Erlenmeyer flasks filled with 20 mL of KNO_3 solutions (0.1 M) and 0.03 g of BCM. The pH values of the KNO_3 solutions were previously adjusted between 2–10.5 with 0.1 M of NaOH and 0.1 M of HCl. After, the KNO_3 solutions were agitated for 24 h, at $24 \text{ }^\circ\text{C}$, and the final pH was measured. The ΔpH (final pH – initial pH) versus initial pH was plotted for the determination of the pH_{PZC} . FTIR analyses were employed to predict the functional groups present on the surface of BCM and how they interact with RhB during biosorption. The samples of BCM were prepared using the KBr disk method, and the transmission FTIR spectra were recorded in the 4000 and 400 cm^{-1} (Shimadzu IRAffinity-1 spectrophotometer).

Batch biosorption experiments

The batch adsorption experiments were conducted with 150 mL Erlenmeyer flasks containing 50 mL RhB aqueous solutions. The flasks were agitated using an incubator shaker at 150 rpm. The influence of some physicochemical parameters on the adsorption process was evaluated as follows: pH (2, 4, 6, 8, and 10), initial RhB concentration (20.0, 50.0, 100.0, 150.0, 200.0 mg L^{-1}), biosorbent dosage (0.5, 1.0, 1.5, 2.0, 3.0 g L^{-1}), and temperature (20, 30, and $40 \text{ }^\circ\text{C}$). All biosorption experiments were performed in triplicate. The residual RhB concentration in the solution was determined using an UV–Vis spectrophotometer (Hach DR6000, $\lambda_{\text{max}} = 554$

nm) after the removal of biosorbent by filtration. The amounts of RhB adsorbed by biosorbent, q_e (mg g^{-1}), and RhB removal efficiency, R (%), were calculated according to Eqs. (1) and (2), respectively:

$$q_e = \frac{(C_i - C_e) \cdot B}{B} \quad (1)$$

$$R(\%) = \frac{C_i - C_e}{C_i} \times 100 \quad (2)$$

where C_i and C_e are the initial and the equilibrium RhB concentrations (mg L^{-1}) and B is the biosorbent concentration in solution (g L^{-1}).

Column biosorption experiment

The performance of the BCM was investigated in a continuous mode using an up-flow fixed-bed glass column (height = 20 cm, internal diameter = 1.0 cm). The column was packed with 2.0 g of BCM between two glass wool layers, providing an initial bed height of 6.8 cm. A peristaltic pump was used to pump RhB solution upward through the bed. Experiments were performed at room temperature (25–27 °C). The column was fed with 50 mg L^{-1} RhB solution at a flow rate of 4 mL min^{-1} .

Error analysis

In order to evaluate the performance of different models in fitting to data, the root mean square error (RMSE) was determined as Eq. (3):

$$RMSE = \sqrt{\frac{1}{n} \sum (q_{exp} - q_{cal})^2} \quad (3)$$

where q_{exp} and q_{cal} are the experimental and calculated values, and n is the number of samples.

RESULTS AND DISCUSSION

FTIR analysis

The FTIR spectra for BCM before and after RhB adsorption are presented in Figure 1. The broadband observed in BCM spectrum in the region of 3000–3700 cm^{-1} is related to O–H stretching from the hydroxyl groups of polysaccharides (TEIXEIRA et al., 2018). The peak at 2900 cm^{-1} is assigned to the C–H stretching vibrations of aliphatic groups.

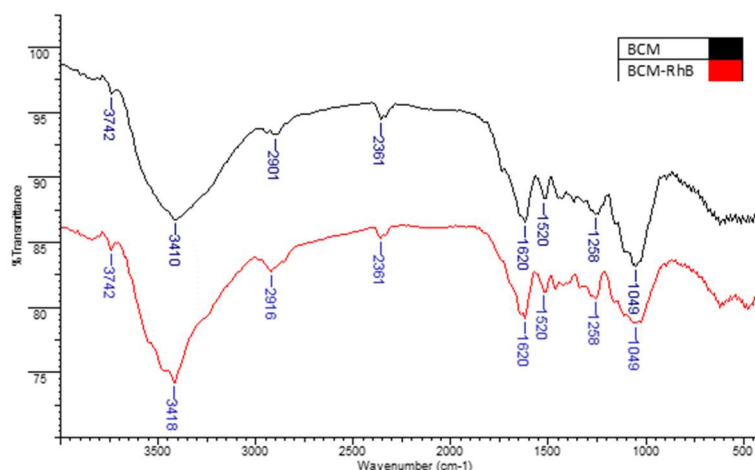


Figure 1: FTIR spectra of BCM and BCM after RhB adsorption (BCM-RhB).

The peaks at 1620 and 1519 cm^{-1} are related to the aromatic skeletal stretching vibrations ($\text{C}=\text{C}$) in lignin. The peak at 1249 cm^{-1} is attributed to $\text{C}-\text{O}$ stretching vibrations. The band at 1049 cm^{-1} can be attributed to $\text{C}-\text{O}-\text{C}$ stretching of glycosidic ring present in the starch chain (GHOSH et al., 2018). After RhB adsorption, alteration in the intensity band of $\text{O}-\text{H}$ stretching vibration ($3800\text{-}3000 \text{ cm}^{-1}$) was detected. Furthermore, the peaks at 1249 cm^{-1} ($\text{C}-\text{O}$) and 2900 cm^{-1} ($\text{C}-\text{H}$) shifted to 1257 and 2916 cm^{-1} , respectively. The changes in these bands indicate the possibility of BCM interaction with RhB molecules via these functional groups.

pH_{pzc} and effect of pH

The point of zero charge (pH_{pzc}) is the pH value where the net charge on the surface of a material is zero. When the $\text{pH}_{\text{pzc}} < \text{pH}$ of the solution, the surface of the adsorbent will be negatively charged. When the $\text{pH}_{\text{pzc}} > \text{pH}$ of the solution, the adsorbent's surface will be positively charged. According to the plot of ΔpH versus initial pH (Fig 2a), the pH_{pzc} for BCM was found to be 5.88.

The pH determines the adsorbent's surface charge and the solubility of adsorbates (SANTOS et al., 2019). Therefore, it was monitored during the adsorption experiments. According to Fig 2b, when the pH value was from 2.0 to 10.0, the RhB removal decreased from 79.3 to 61.6%. At $\text{pH} < \text{pH}_{\text{pzc}} (=5.88)$, the BCM surface is expected to be predominantly positively due to the protonation of surface functional groups. In the same condition, RhB exists in cationic and monomeric forms (ZAIDI et al., 2018). Although the cationic form of RhB competes with the H^+ ions at low pH, it was observed that the removal of RhB was higher in acid conditions. This suggests that electrostatic interaction might not be the primary mechanism of the RhB adsorption onto BCM. The monomeric form RhB is smaller in size and may enter easily into the micropore of the biosorbent, contributing to higher removal values in acid conditions. At $\text{pH} > 4$, RhB exists as zwitterionic forms that can lead to the aggregation of the dye to form larger molecules that are unable to enter the micropores (CHEN et al., 2019).

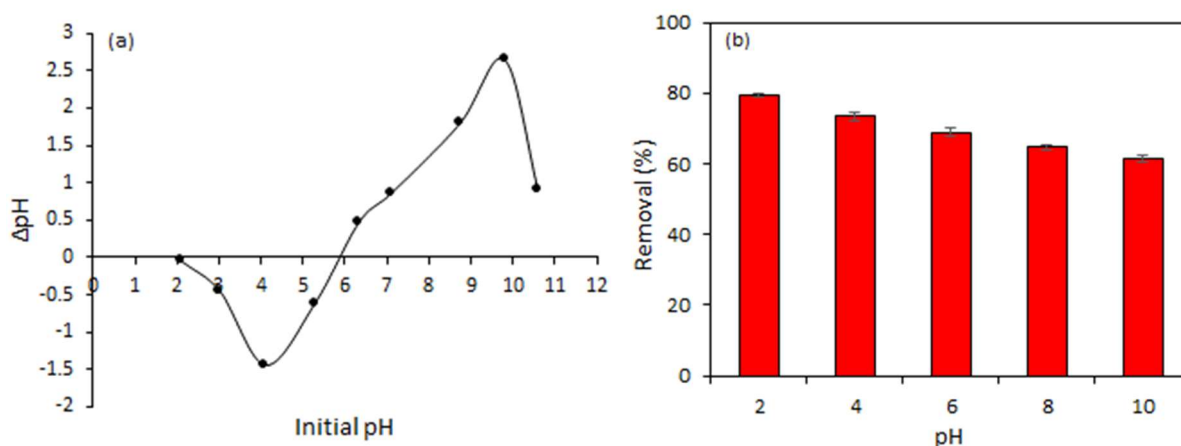


Figure 2: (a) Point of zero charge (pH_{pzc}) of BCM; (b) Effect of pH on the RhB removal by BCM (biosorbent dosage = 1.0 g L^{-1} , $[\text{RhB}] = 50 \text{ mg L}^{-1}$, contact time = 120 min, temperature = 30 $^{\circ}\text{C}$).

Effect of biosorbent dosage

The RhB removal increased from 51.0 to 98.7% when the biosorbent dosage rose from 0.5 to 3.0 g/L (Figure 3). This was expected because the surface area and the number of free active adsorption sites raised with an increase in the BCM amount, increasing the amount of adsorbed dye. On the other hand, the adsorption capacity decreased from 45.2 to 14.6 mg/g, when the biosorbent dosage varied from 0.5 to 3.0 g/L, which is explained by adsorption active sites that remained unsaturated during the adsorption reaction.

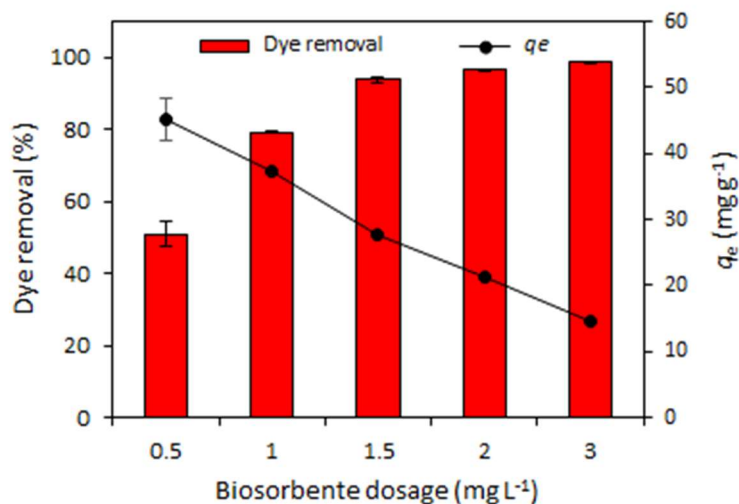


Figure 3: Effect of biosorbent dosage on the RhB removal by BCM (pH = 2.0, [RhB] = 50 mg L⁻¹, contact time = 120 min, temperature = 30 °C).

Effect of contact time and kinetics modelling

The ideal adsorbent should quickly adsorb the adsorbate from the liquid phase and establish the equilibrium. Figure 4a shows the RhB adsorption by BCM at different contact times and temperatures. Rapid adsorption of dye occurred during the first 10 min for three temperatures and was gradually slowed down until 120 min. The rapid biosorption of the RhB in the first 10 min is attributed to the high number of free active sites on the adsorbent surface. Also, it can be seen that the biosorption capacity of BCM increased from 40.57 to 56.15 mg g⁻¹ when the temperature was increased from 20 to 40 °C, indicating that an endothermic process controls the biosorption of RhB onto BCM.

The determination of kinetic parameters is relevant to achieve the optimization of the process. Kinetic studies of RhB removal by BCM were performed with a constant initial dye concentration (50 mg L⁻¹), 0.5 g L⁻¹ biosorbent, at temperatures of 20, 30, and 40°C. Three well established kinetic models, the pseudo-first-order model (LAGERGREN, 1898), pseudo-second-order model (HO et al., 1999), and intraparticle diffusion model (WEBER et al., 1963) were employed to describe the experimental data. The models are expressed as Eqs. (4) through (6), respectively:

$$q_t = q_e(1 - e^{-K_1 t}) \quad (4)$$

$$q_t = \frac{K_2 q_e^2 t}{1 + K_2 q_e t} \quad (5)$$

$$q_t = K_{id} t^{1/2} + C \quad (6)$$

where q_e and q_t represent the amounts of RhB adsorbed by BCM (mg g⁻¹) at equilibrium and at time t , respectively. K_1 ,

K_2 , and K_{id} are the pseudo-first-order rate constant (min^{-1}), pseudo-second-order rate constant ($\text{g mg}^{-1} \text{min}^{-1}$), and intraparticle diffusion rate constant ($\text{mg g}^{-1} \text{min}^{-0.5}$), respectively. C (mg g^{-1}) is the intercept, which is related to the thickness of the boundary layer.

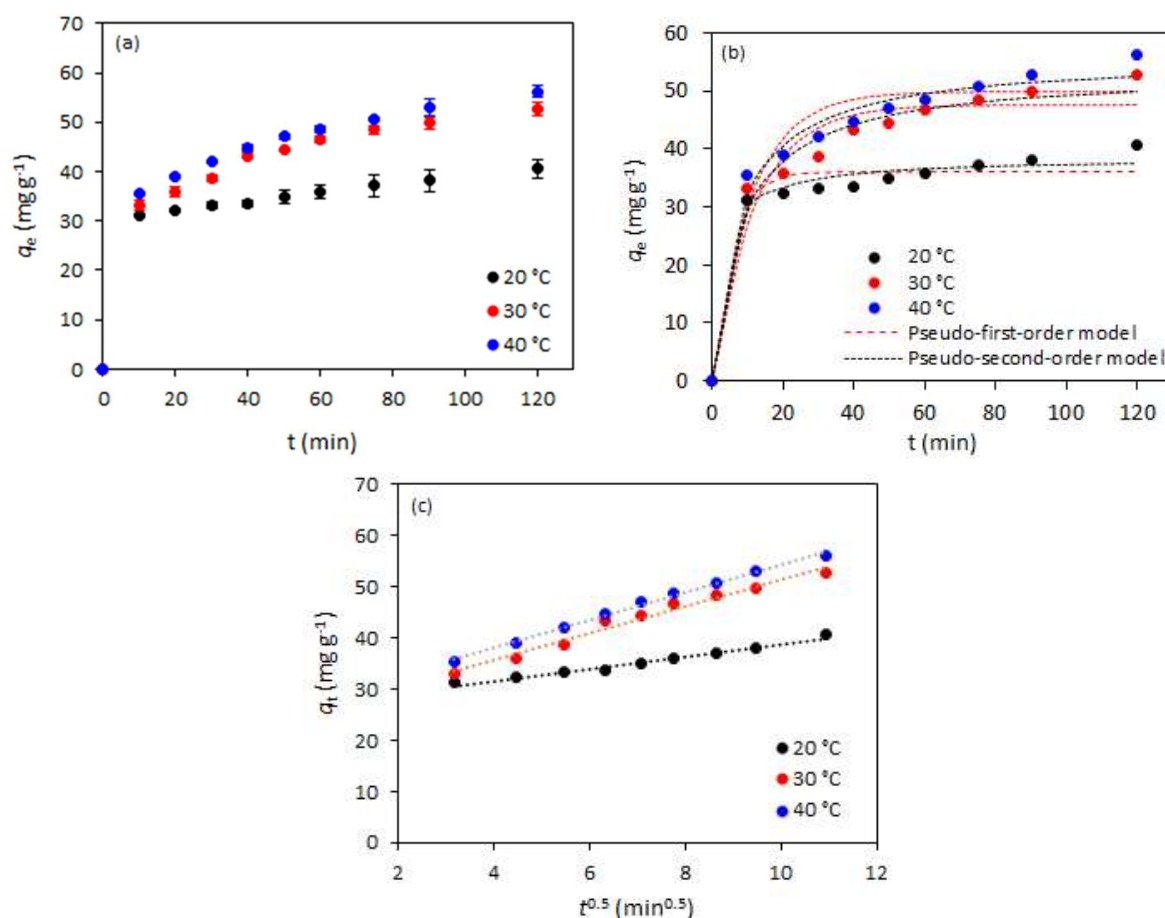


Figure 4: (a) Effect of contact time and temperature on the RhB removal by BCM ($\text{pH} = 2.0$, $[\text{RhB}] = 50 \text{ mg L}^{-1}$, biosorbent dosage = 0.5 g L^{-1}), (b) Plots for pseudo-first-order and pseudo-second-order kinetic models; (c) Plot for intraparticle diffusion kinetic model.

The kinetic parameters, R^2 , and $RMSE$ calculated from the kinetic models are summarized in Table 1. Both pseudo-first-order and pseudo-second-order models resulted in good fits (Fig 4b). However, the pseudo-second-order model displayed higher R^2 , lower $RMSE$ values, and the calculated q_e is closest to experimental q_e . Thus, these results suggest that the pseudo-second-order model provided a good correlation for the biosorption of RhB on BCM. The intraparticle diffusion model was used to identify the possible mechanism involved in the biosorption process. As seen in Figure 4c, the plots did not cross the origin ($C \neq 0$), suggesting that the intraparticle diffusion is not the only operative mechanism. Therefore, the biosorption of RhB onto BCM was controlled by both intraparticle diffusion and surface processes.

Table 1: Kinetic parameters estimated by the pseudo first-order, pseudo second-order and intraparticle diffusion models for the RhB biosorption on BCM, at different temperatures.

Model	Temperature ($^{\circ}\text{C}$)		
	20	30	40
$q_{\text{experimental}}$ (mg g^{-1})	40.57	52.65	56.15
Pseudo-first-order			
q_1 (mg g^{-1})	36.00	47.55	49.90
k_1 (min^{-1})	0.179	0.088	0.090
R^2	0.957	0.944	0.943
$RMSE$	2.355	3.586	3.813
Pseudo-second-order			

q_2 (mg g ⁻¹)	38.40	53.30	55.80
k_2 (g mg ⁻¹ min ⁻¹)	8.3×10^{-3}	2.2×10^{-3}	2.3×10^{-3}
R^2	0.979	0.981	0.981
RMSE	2.107	1.654	2.239
Intraparticle diffusion			
K_{id} (mg g ⁻¹ min ^{-0.5})	1.206	2.626	2.696
C (mg g ⁻¹)	26.72	25.17	27.31
R^2	0.976	0.978	0.995
RMSE	0.439	0.914	0.432

Effect of dye concentration and isotherm modelling

As shown in Figure 5a, despite the decrease in dye removal efficiency when the initial RhB concentration increased from 20 to 200 mg/l, the q_e of RhB adsorbed by BCM increased from 30.7 to 97.9 mg g⁻¹. This is attributed to a high mass transfer driving force at high initial dye concentrations (WU et al., 2020).

The adsorption isotherms provide information about the interaction mechanism between adsorbate and adsorbent at equilibrium and maximum adsorption capacity of a specific adsorbent (SANTOS et al., 2019). In this study, the equilibrium experiments were conducted with different initial RhB concentrations (20-200 mg L⁻¹), 0.5 g biosorbent L⁻¹ at 40 °C. Three different isotherms models were applied: Langmuir (LANGMUIR, 1918), Freundlich (FREUNDLICH, 1906) and Dubinin-Radushkevich (D-R) (DUBININ et al., 1947). The Langmuir and Freundlich models are presented as Eqs. (7) and (8), respectively:

$$q_e = \frac{q_{max}K_L C_e}{1+K_L C_e} \quad (7)$$

$$q_e = K_F C_e^{1/n} \quad (8)$$

where q_e (mg g⁻¹) is the amount of RhB adsorbed by the BCM at the equilibrium, C_e (mg L⁻¹) is the RhB concentration in the solution at the equilibrium, q_{max} (mg g⁻¹) is the maximum adsorption capacity of BCM, K_L (L mg⁻¹) is the Langmuir constant, K_F ((mg g⁻¹)(mg L⁻¹)^{-1/n}) is the Freundlich constant, and n (dimensionless) is the intensity of adsorption.

The Langmuir isotherm model assumes that each molecule of adsorbate interacts with the individual active site from the adsorbent surface and form a homogeneous monolayer. The Freundlich isotherm model suggests that adsorption occurs in multilayer on an energetically heterogeneous surface. Based on the R^2 and RMSE calculated from the isotherm models (Table 2), it could be concluded that the adsorption data were best fitted to the Langmuir model. Therefore, the adsorption of RhB occurs as a monolayer on the surface of BCM, and the maximum adsorption capacity was estimated to be 111.52 mg g⁻¹. Table 3 compared the maximum adsorption capacities of RhB by BCM and other raw and treated adsorbents under optimal conditions. The BCM presented a higher adsorption capacity than those obtained for many adsorbents. Another advantage of BCM is that it can be used in natural form without pretreatment.

The D-R isotherm model is presented in Eq. (9). This model is useful to determine the nature of the adsorption process as physical and chemical.

$$q_e = q_m e^{-\beta \varepsilon^2}; \quad \varepsilon = RT \ln \left(1 + \frac{1}{C_e} \right) \quad (9)$$

where q_e (mol g⁻¹) is the amount of RhB adsorbed on the BCM, q_m (mol g⁻¹) is the maximum biosorption capacity, β (mol² kJ⁻²) is the constant related to the mean free energy of biosorption, ε is the Polanyi potential, R (8.314 J mol⁻¹ K⁻¹) is the ideal gas constant, and T (K) is the absolute temperature.

The mean free energy of biosorption (E , kJ mol⁻¹) can be determined using the activity coefficient β , according to Eq. (10):

$$E = \frac{1}{\sqrt{2\beta}} \quad (10)$$

When $E < 8 \text{ kJ mol}^{-1}$, the adsorption process proceeds through a physical mechanism, and in the range from 8 to 16 kJ mol^{-1} , the adsorption process is controlled by a chemical mechanism. As shown in Table 2, the E value of $2.864 \text{ kJ mol}^{-1}$ indicated that RhB was adsorbed onto BCM following a physical process.

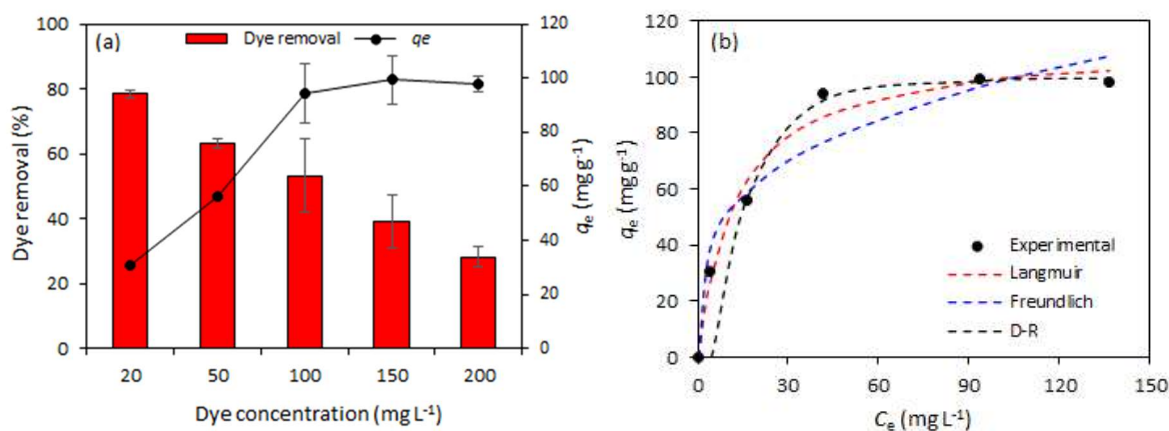


Figure 5: (a) Effect of initial dye concentration on the RhB removal by BCM (pH = 2, biosorbent dosage = 0.5 g L^{-1} , [RhB] = 50 mg L^{-1} , contact time = 120 min, temperature = $40 \text{ }^\circ\text{C}$). (b) Plots for Langmuir, Freundlich and D-R isotherms models.

Table 2: Isotherm parameters for the biosorption of RhB onto BCM.

Model	Parameter (unit)	Value
Langmuir	q_{\max} (mg g^{-1})	111.52
	K_L (L mg^{-1})	0.080
	R^2	0.983
	RMSE	4.928
Freundlich	K_F ($(\text{mg g}^{-1}) (\text{mg L}^{-1})^{-1/n}$)	26.783
	n	3.535
	R^2	0.942
	RMSE	9.144
D-R	q_m (mg g^{-1})	100.66
	E (kJ mol^{-1})	2.864
	R^2	0.750
	RMSE	12.582

Table 3: Maximum adsorption capacity of RhB onto BCM and other adsorbents under optimal conditions.

Adsorbent	q_{\max} (mg g^{-1})	Reference
Babassu coconut mesocarp (BCM)	111.52	This work
Cassava slag biochar	105.30	(WU et al., 2020)
Plantain peel activated biochar	84.41	(ADEKOLA et al., 2019)
Bamboo shoot shells biochar	85.80	(HOU et al., 2019)
Furfural residue	37.93	(CHEN et al., 2019)
<i>Casuarina equisetifolia</i> needles	82.34	(KOOH et al., 2016)
Earthworm manure biochar	21.60	(WANG et al., 2017)

Thermodynamics studies

The thermodynamics parameters of RhB biosorption onto BCM, *i.e.*, Gibbs free energy change (ΔG), entropy (ΔS), and enthalpy (ΔH) were determined using the Eqs. (11) through (13):

$$\Delta G = -RT \ln K_D \quad (11)$$

$$\Delta G = \Delta H - T\Delta S \quad (12)$$

$$\ln K_D = \frac{\Delta S}{R} - \frac{\Delta H}{R} \times \frac{1}{T} \quad (13)$$

where K_D (q_e/C_e) is the distribution coefficient, R is the universal gas constant ($8.314 \text{ J K}^{-1} \text{ mol}^{-1}$), and T (K) is the absolute temperature. Values of ΔH and ΔS could be calculated from the plot of $\ln K_D$ versus $1/T$ (Figure 6).

The calculated thermodynamic parameters are shown in Table 4. The negative values of ΔG suggest that the RhB biosorption onto BCM is thermodynamically spontaneous and feasible at the studied temperatures (20, 30, and 40 °C). The positive ΔH value of 27.48 KJ mol⁻¹ indicates that the biosorption process is endothermic and is facilitated with an increase in temperature. The ΔS was also found to be positive (98.55 J mol⁻¹ K⁻¹), revealing the affinity of the BCM for RhB and showing that the randomness at the solid/solution interface increases during the biosorption of the dye.

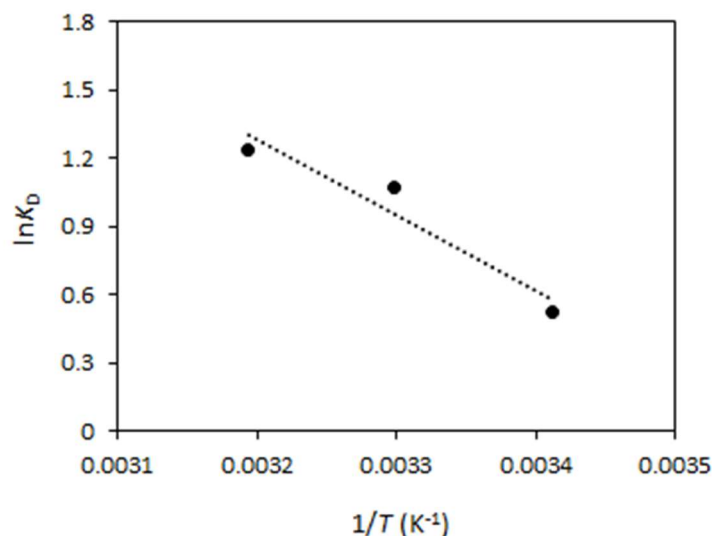


Figure 6: Plot of $\ln K_D$ versus $1/T$ for estimation of thermodynamic parameters.

Table 4: Thermodynamic parameters estimated for RhB biosorption onto BCM.

T (°C)	K _D	ΔG (KJ mol ⁻¹)	ΔH (KJ mol ⁻¹)	ΔS (J mol ⁻¹ K ⁻¹)
20	1.687	-1.42	27.48	98.55
30	2.923	-2.40		
40	3.452	-3.39		

Fixed bed adsorption

Adsorption of dye in full-scale plants is commonly applied in continuous systems, using fixed-bed columns packed with the adsorbent. Thus, an up-flow fixed-bed adsorption experiment was executed to evaluate the performance of the BCM in continuous systems. Figure 5 shows the breakthrough curve obtained from a complete saturation of the column. The breakthrough time (t_b , min, the time equivalent to the $C_t/C_0 = 0.05$) and the exhaustion time (t_e , min, the time equivalent to the $C_t/C_0 = 0.95$) were 611 and 840 min, respectively. The amount of RhB adsorbed onto BCM at equilibrium, q_{eq} (mg g⁻¹) was calculated by Eq. (14):

$$q_{eq} = \frac{FC_0}{1000 m_{ads}} \int_0^{t_{total}} \left(1 - \left(\frac{C_t}{C_0} \right) \right) dt \quad (14)$$

where F is the volumetric flow (mL min⁻¹), C_0 is the RhB concentration in affluent (mg L⁻¹), and m_{ads} is the biosorbent mass (g).

Yan model (YAN et al., 2001) and Yoon-Nelson model (YOON et al., 1984) were applied to describe the experimental data of the fixed-bed column. These models are described by Eqs. (15) and (16), respectively:

$$\frac{C_t}{C_0} = 1 - \frac{1}{1 + \left(\frac{C_0 F}{q_{Ya} m}\right)^{\alpha_{Ya}}} \quad (15)$$

$$\frac{C_t}{C_0} = \frac{1}{(1 + \exp(K_{YN}\tau - K_{YN}t))} \quad (16)$$

where q_{Ya} is the maximum adsorption capacity (mg g^{-1}), α_{Ya} is an empirical parameter, F is the volumetric flow (min mL^{-1}), m is the biosorbent mass (g), K_{YN} is the kinetic constant of Yoon-Nelson, and τ is the time required to achieve 50% saturation of the column.

Based on values of R^2 and $RMSE$, it was observed that both models described the experimental data with excellent accuracy (Figure 7, Table 5). Yan model was able to predict the adsorption capacity with a variation of only 0.41%. Yoon-Nelson model was able to predict the τ with a deviation of 0.33%.

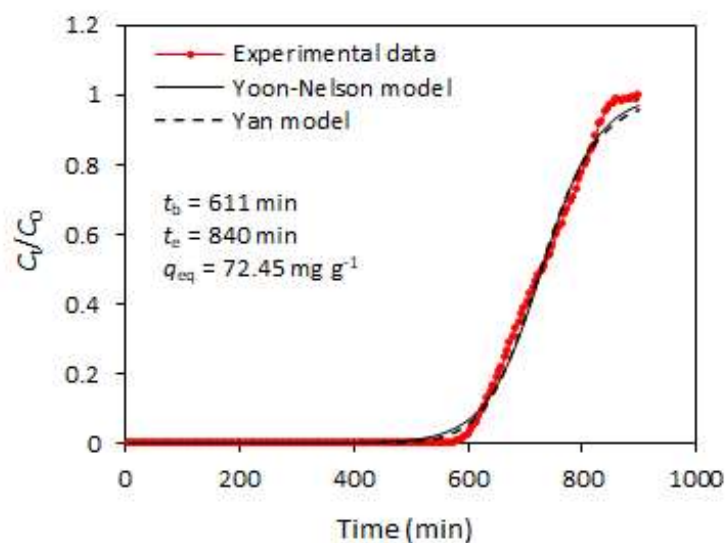


Figure 7: Breakthrough curve of RhB biosorption onto BCM (solution pH = 2, $F = 4.0 \text{ mL min}^{-1}$, $C_0 = 50 \text{ mg L}^{-1}$, $m_{\text{ads}} = 2 \text{ g}$).

Table 5: Breakthrough parameters for RhB biosorption on BCM.

Model	Parameter (unit)	Value
Yan	α_{Ya}	14.751
	q_{Ya}	72.75
	q	72.45
	R^2	0.996
	$RMSE$	0.022
Yoon-Nelson	$K_{YN} (\text{min}^{-1})$	0.020
	$\tau (\text{min})$	729.92
	$\tau_{\text{exp}} (\text{min})$	732.35
	R^2	0.996
	$RMSE$	0.021

CONCLUSIONS

This study shows that BCM is an effective biosorbent for the removal of RhB from aqueous solution. The biosorption kinetic data and equilibrium data were best described by pseudo-second-order model and Langmuir isotherm model, respectively. The maximum adsorption capacity was estimated at 111.52 mg g^{-1} (at $40 \text{ }^\circ\text{C}$). Thermodynamic parameters indicated that the RhB biosorption onto BCM was physical, spontaneous, and facilitated with the rise in temperature. Continuous system conducted in an up-flow fixed-bed column fed confirmed the applicability of BCM on a commercial-scale. The breakthrough data were well fitted to Yan and Yoon-Nelson models, and maximum uptake and breakthrough time were reported as 72.45

mg g⁻¹ and 611 min, respectively.

REFERENCES

- ADEKOLA, F. A.; AYODELE, S. B.; INYINBOR, A. A.. Activated biochar prepared from plaintain peels: Characterization and Rhodamine B adsorption data set. **Chemical Data Collections**, v.19, p.100170, 2019. DOI: <http://doi.org/10.1016/j.cdc.2018.11.012>
- BELLO, O. S.; ALAO, O. C.; ALAGBADA, T. C.; OLATUNDE, A. M.. Biosorption of ibuprofen using functionalized bean husks. **Sustainable Chemistry and Pharmacy**, v.13, p.100151, 2019. DOI: <http://doi.org/10.1016/j.scp.2019.100151>
- CASTRO, K. C.; COSSOLIN, A. S.; REIS, H. C. O.; MORAIS, E. B.. Biosorption of anionic textile dyes from aqueous solution by yeast slurry from brewery. **Brazilian Archives of Biology and Technology**, v.60, p.1-13, 2017. DOI: <http://doi.org/10.1590/1678-4324-2017160101>
- CHEN, X., LI, H.; LIU, W.; ZHANG X.; WU, Z.; BI, S.; ZHANG, W.; ZHAN, H.. Effective removal of methyl orange and rhodamine B from aqueous solution using furfural industrial processing waste: Furfural residue as an eco-friendly biosorbent. **Colloids and Surfaces A: Physicochemical and Engineering Aspects**, v.583, p.123976, 2019. DOI: <http://doi.org/10.1016/j.colsurfa.2019.123976>
- DAHRI, M. K.; KOOH, M. R. R.; LIM, L. B. L.. Water remediation using low cost adsorbent walnut shell for removal of malachite green: Equilibrium, kinetics, thermodynamic and regeneration studies. **Journal of Environmental Chemical Engineering**, v.2, n.3, p.1434–1444, 2014. DOI: <http://doi.org/10.1016/j.jece.2014.07.008>
- DANESHVAR, E.; VAZIRZADEH, A.; NIAZI, A.; SILLANPÄÄ, M.; BHATNAGAR, A.. A comparative study of methylene blue biosorption using different modified brown, red and green macroalgae: Effect of pretreatment. **Chemical Engineering Journal**, v.307, p.435–446, 2017. DOI: <http://doi.org/10.1016/j.cej.2016.08.093>
- DENIZ, F.; KEPEKCI, R. A.. Bioremoval of Malachite green from water sample by forestry waste mixture as potential biosorbent. **Microchemical Journal**, v.132, p.172–178, 2017. DOI: <http://doi.org/10.1016/j.microc.2017.01.015>
- DUBININ, M. M.; RADUSHKEVICH, L. V.. Equation of the characteristic curve of activated charcoal. **Proceedings of the USSR Academy Sciences**, v.55, p.331–333, 1947.
- EL MESSAOUDI, N.; EL HHOMRI, M.; DBIK, A.; BENTAHAR, S.; LACHERAI, A.; BAKIZ, B.. Biosorption of Congo red in a fixed-bed column from aqueous solution using jujube shell: Experimental and mathematical modeling. **Journal of Environmental Chemical Engineering**, v.4, n.4, p.3848–3855, 2016. DOI: <http://doi.org/10.1016/j.jece.2016.08.027>
- FIDELES, R. A.; TEODORO, F. S.; XAVIER, A. L. P.; ADARME, O. F. H.; GIL, L. F.; GURGEL, L. V. A.. Trimellitated sugarcane bagasse: A versatile adsorbent for removal of cationic dyes from aqueous solution. Part II: Batch and continuous adsorption in a bicomponent system. **Journal of Colloid and Interface Science**, v.552, p.752–763, 2019. DOI: <http://doi.org/10.1016/j.jcis.2019.05.089>
- FREUNDLICH, H.. Über die Adsorption in Lösungen. **Zeitschrift Für Physikalische Chemie**, v.57, p.385-470, 1906.
- SEGURA, S. G.; BRILLAS, E.. Combustion of textile monoazo, diazo and triazo dyes by solar photoelectro-Fenton: Decolorization, kinetics and degradation routes. **Applied Catalysis B: Environmental**, v.181, p.681–691, 2016. DOI: <http://doi.org/10.1016/j.apcatb.2015.08.042>
- GEBRATI, L.; EL ACHABY, M.; CHATOUI, H.; LAQBAQBI, M.; EL KHARRAZ, J.; AZIZ, F.. Inhibiting effect of textile wastewater on the activity of sludge from the biological treatment process of the activated sludge plant. **Saudi Journal of Biological Sciences**, v.26, n.7, p.1753–1757, 2019. DOI: <http://doi.org/10.1016/j.sjbs.2018.06.003>
- GHOSH, A.; SANTOS, A. M. S.; CUNHA, J. R.; DASGUPTA, A.; FUJISAWA, K.; FERREIRA, O. P.; LOBO, A. O.; TERRONES, M.; TERRONES, H.; VIANA, B. C.. CO₂ Sensing by in-situ Raman spectroscopy using activated carbon generated from mesocarp of babassu coconut. **Vibrational Spectroscopy**, v.98, p.111–118, 2018. DOI: <http://doi.org/10.1016/j.vibspec.2018.07.014>
- HO, Y.; MCKAY, G.. Pseudo-second order model for sorption processes. **Process Biochemistry**, v.34, n.5, p.451–465, 1999. DOI: [http://doi.org/10.1016/S0032-9592\(98\)00112-5](http://doi.org/10.1016/S0032-9592(98)00112-5)
- HOPPEN, M. I.; CARVALHO, K. Q.; FERREIRA, R. C.; PASSIG, F. H.; PERERIRA, I. C.; RIZZO-DOMINGUES, R. C. P.; LENZI, M. K.; BOTTINI, R.. Adsorption and desorption of acetylsalicylic acid onto activated carbon of babassu coconut mesocarp. **Journal of Environmental Chemical Engineering**, v.7, n.1, p.102862, 2019. DOI: <http://doi.org/10.1016/j.jece.2018.102862>
- HOU, Y.; HUANG, G.; LI, J.; YANG, Q.; HUANG, S.; CAI, J.. Hydrothermal conversion of bamboo shoot shell to biochar: Preliminary studies of adsorption equilibrium and kinetics for rhodamine B removal. **Journal of Analytical and Applied Pyrolysis**, v.143, p.104694, 2019. DOI: <http://doi.org/10.1016/j.jaap.2019.104694>
- KOOH, M. R. R.; DAHRI, M. K.; LIM, L. B. L.. The removal of rhodamine B dye from aqueous solution using Casuarina equisetifolia needles as adsorbent. **Cogent Environmental Science**, v.2, n.1, 2016. DOI: <http://doi.org/10.1080/23311843.2016.1140553>
- LAGERGREN, S. Y.. Zur theorie der sogenannten adsorption gelöster stoffe, kungliga svenska vetenskapsakademiens. **Handlingar**, v.24, p.1–39, 1898.
- LANGMUIR, I.. The adsorption of gases on plane surfaces of glass, mica and platinum. **Journal of American Chemical Society**, v.40, p.1361-1402, 1918.
- LIU, M.; CHEN, Q.; LU, K.; HUANG, W.; LÜ, Z.; ZHOU, C.; YU, S.; GAO, C.. High efficient removal of dyes from aqueous solution through nanofiltration using diethanolamine-modified polyamide thin-film composite membrane.

Separation and Purification Technology, v.173, p.135–143, 2017. DOI: <http://doi.org/10.1016/j.seppur.2016.09.023>

NASCIMENTO, J. M.; OLIVEIRA, J. D.; LEITE, S. G. F.. Chemical characterization of biomass flour of the babassu coconut mesocarp (*Orbignya speciosa*) during biosorption process of copper ions. **Environmental Technology and Innovation**, v.16, p.100440, 2019. DOI: <http://doi.org/10.1016/j.eti.2019.100440>

NOVOTNÝ, Č.; DIAS, N.; KAPANEN, D.; MALACHOVÁ, K.; VÁNDROVCOVÁ, M.; ITÄVAARA, M.; LIMA, N.. Comparative use of bacterial, algal and protozoan tests to study toxicity of azo- and anthraquinone dyes. **Chemosphere**, v.63, n.9, p.1436–1442, 2006. DOI: <http://doi.org/10.1016/j.chemosphere.2005.10.002>

PARVIN, F.; FERDAUS, Z.; TAREQ, S. M.; CHOUDHURY, T. R.; ISLAM, J. M. M.; KHAN, M. A.. Effect of gamma-irradiated textile effluent on plant growth. **International Journal of Recycling of Organic Waste in Agriculture**, v.4, n.1, p.23–30, 2015. DOI: <http://doi.org/10.1007/s40093-014-0081-z>

SANTAEUFEMIA, S.; TORRES, E.; ABALDE, J.. Biosorption of ibuprofen from aqueous solution using living and dead biomass of the microalga *Phaeodactylum tricornutum*. **Journal of Applied Phycology**, v.30, n.1, p.471–482, 2018. DOI: <http://doi.org/10.1007/s10811-017-1273-5>

SANTOS, B. A. P.; COSSOLIN, A. S.; REIS, H. C. O.; CASTRO, K. C.; SILVA, E. R.; PERERIRA, G. M.; SOUZA JUNIOR, P. T.; DALL'OGGIO, E. L.; VASCONCELOS, L. G.; MORAIS, E. B.. Baker's yeast-MnO₂ composites as biosorbent for Malachite green: An ecofriendly approach for dye removal from aqueous solution. **Environment and Water Magazine**, v.14, p.1-15, 2019. DOI: <http://doi.org/10.4136/ambi-agua.2254>

SETHULEKSHMI, S.; CHAKRABORTY, S.. Textile wastewater treatment using horizontal flow constructed wetland and effect of length of flow in operation efficiency. **Journal of Environmental Chemical Engineering**, v.9, n.6, p.106379, 2021. DOI: <http://doi.org/10.1016/j.jece.2021.106379>

WANG, Z.; SHEN, D.; SHEN, F.; WU, C.; GU, S.. Kinetics, equilibrium and thermodynamics studies on biosorption of Rhodamine B from aqueous solution by earthworm manure derived biochar. **International Biodeterioration and Biodegradation**, v.120, p.104–114, 2017. DOI: <http://doi.org/10.1016/j.ibiod.2017.01.026>

TAN, D.; BAI, B.; JIANG, D.; SHI, L.; CHENG, S.; TAO, D.; JI, S.. Rhodamine B induces long nucleoplasmic bridges and other nuclear anomalies in *Allium cepa* root tip cells. **Environ Sci Pollut Res Int.**, v.21, n.5, p.3363–3370, 2014. DOI: <http://doi.org/10.1007/s11356-013-2282-9>

TANVEER, R.; YASAR, A.; TABINDA, A. B.; IKLAQ, A.; NISSAR, H.; NIZAMI, S.. Comparison of ozonation, Fenton, and photo-Fenton processes for the treatment of textile dye-bath effluents integrated with electrocoagulation. **Journal of Water Process Engineering**, v.46, p.102547, 2022. DOI: <http://doi.org/10.1016/j.jwpe.2021.102547>

TEIXEIRA, I. R.; VERNASQUI, L. G.; SAI N. B. P.; MEDEIROS, F. V. S.. Adsorção de azul de metileno por meio de resíduos de *Poincianella pluviosa* var. *peltophoroides* (Benth.) L.P. Queiroz. **Iberoamerican Journal of Environmental Sciences**, v.12, p.297-306, 2021. DOI: <http://doi.org/10.6008/CBPC2179-6858.2021.006.0025>

TEIXEIRA, P. R. S.; TEIXEIRA, A. S. M. M.; FARIAS, E. A. O.; SILVA, D. A.; NUNES, L. C. C.; LEITE, C. M. S.; SILVA FILHO, E. C.; EIRAS, C.. Chemically modified babassu coconut (*Orbignya* sp.) biopolymer: characterization and development of a thin film for its application in electrochemical sensors. **Journal of Polymer Research**, v.25, n.5, 2018. DOI: <http://doi.org/10.1007/s10965-018-1520-8>

TRIPATY, N. K.; NABI, M. J.; SAHU, G. P.; KUMAR, A. A.. Genotoxicity testing of two red dyes in the somatic and germ line cells of *Drosophila*. **Food and Chemical Toxicology**, v.33, p.923–927, 1995.

TUNÇ, Ö.; TANACI, H.; AKSU, Z.. Potential use of cotton plant wastes for the removal of Remazol Black B reactive dye. **Journal of Hazardous Materials**, v.163, n.1, p.187–198, 2009. DOI: <http://doi.org/10.1016/j.jhazmat.2008.06.078>

VIEIRA, A. P.; SANTANA, S. A. A.; BEZERRA, C. W. B.; SILVA, H. A. S.; CHAVES, J. A. P.; MELO, J. C. P.; SILVA FILHO, E. C.; Epicarp and Mesocarp of Babassu (*Orbignya speciosa*): Characterization and Application. **Journal of the Brazilian Chemical Society**, v.22, n.1, p.21–29, 2011. DOI: <http://doi.org/10.1590/S0103-50532011000100003>

WEBER, W. J.; MORRIS, J. C.. Kinetics of adsorption on carbon from solution. **Journal of the Sanitary Engineering Division**, v.89, p.31-60, 1963.

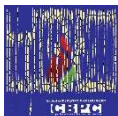
WU, J.; YANG, J.; HUANG, G.; XU, C.; LIN, B.. Hydrothermal carbonization synthesis of cassava slag biochar with excellent adsorption performance for Rhodamine B. **Journal of Cleaner Production**, v.251, p.119717, 2020. DOI: <http://doi.org/10.1016/j.jclepro.2019.119717>

YAN, G.; VIRARAGHAVAN, T.; CHEN, M.. A new model for heavy metal removal in a biosorption column. **Adsorption Science and Technology**, v.19, n.1, p.25–43, 2001. DOI: <http://doi.org/10.1260/0263617011493953>

YOON, Y. H.; NELSON, J. H.. Application of Gas Adsorption Kinetics I. A Theoretical Model for Respirator Cartridge Service Life. **American Industrial Hygiene Association Journal**, v.45, n.8, p.509–516, 1984. DOI: <http://doi.org/10.1080/15298668491400197>

ZAIDI, N. A. H.; LIM, L. B. L.; PRYANTHA, N.; USMAN, A.. *Artocarpus odoratissimus* Leaves as an Eco-friendly Adsorbent for the Removal of Toxic Rhodamine B Dye in Aqueous Solution: Equilibrium Isotherm, Kinetics, Thermodynamics and Regeneration Studies. **Arabian Journal for Science and Engineering**, v.43, n.11, p.6011–6020, 2018. DOI: <http://doi.org/10.1007/s13369-018-3228-9>

Todas as obras (artigos) publicadas serão tokenizadas, ou seja, terão um NFT equivalente armazenado e comercializado livremente na rede OpenSea (https://opensea.io/HUB_CBPC), onde a CBPC irá operacionalizar a transferência dos direitos materiais das publicações para os próprios autores ou quaisquer interessados em adquiri-los e fazer o uso que lhe for de interesse.



Os direitos comerciais deste artigo podem ser adquiridos pelos autores ou quaisquer interessados através da aquisição, para posterior comercialização ou guarda, do NFT (Non-Fungible Token) equivalente através do seguinte link na OpenSea (Ethereum).

The commercial rights of this article can be acquired by the authors or any interested parties through the acquisition, for later commercialization or storage, of the equivalent NFT (Non-Fungible Token) through the following link on OpenSea (Ethereum).



<https://opensea.io/assets/ethereum/0x495f947276749ce646f68ac8c248420045cb7b5e/44951876800440915849902480545070078646674086961356520679561157619685359878145>